Development 140, 454-458 (2013) doi:10.1242/dev.085241

Electroporation-mediated somatic transgenesis for rapid functional analysis in insects

Toshiya Ando and Haruhiko Fujiwara*

SUMMARY

Transgenesis is a powerful technique for determining gene function; however, it is time-consuming. It is virtually impossible to carry out in non-model insects in which egg manipulation and screening are difficult. We have established a rapid genetic functional analysis system for non-model insects using a low-cost electroporator (costing under US$200) designed for somatic transformation with the *piggyBac* transposon. Using this system, we successfully generated somatic transgenic cell clones in various target tissues (e.g. olfactory neurons, wing epidermis, larval epidermis, muscle, fat body and trachea) of the silkworm *Bombyx mori* during development. We also induced stable and transient RNA interference (RNAi) using short hairpin RNA (shRNA)-mediating DNA vectors and direct transfer of small interfering RNAs (siRNAs), respectively. We found that these electroporation-mediated approaches could also be applied to the swallowtail butterfly *Papilio xuthus* and the red flour beetle *Tribolium castaneum*. Thus, this method could be a powerful genetic tool for elucidating various developmental phenomena in non-model insects.

KEY WORDS: *In vivo* electroporation, *piggyBac*, Non-model organism

INTRODUCTION

Reverse genetics and transgenic techniques are powerful methods for elucidating gene functions. However, such methods are available for only a few model organisms. Over the recent decades, because of its simplicity, RNA interference (RNAi) has been used as an alternative method for knocking out specific genes. RNAi has enabled *in vivo* functional analyses of specific genes in various non-model organisms (Tomoyasu et al., 2005; Moczek and Rose, 2009). However, several technical obstacles persist, such as low efficiency of the introducing dsRNA in some species (Tomoyasu et al., 2008) and the need for gain-of-function analysis when investigating gene function. To overcome such problems, we decided to directly introduce plasmid DNA into tissues *in vivo* using electroporation and insert exogenous DNA into host chromosomes using the *piggyBac* transposon. We designed a simple electroporator that costs under US$200 (supplementary material Figs S1, S2). Here, we demonstrate that exogenous DNA can be readily introduced into various tissues of the silkworm *Bombyx mori* after embryogenesis using electroporation, and that it can be stably maintained until adulthood. We also successfully induced RNAi using short-hairpin RNA (shRNA)-mediating DNA vectors. These methods were applicable to two other insect species: swallowtail butterfly *Papilio xuthus* and red flour beetle *Tribolium castaneum*. This suggests that our approach could be a powerful tool for rapid *in vivo* functional analysis in a broad range of insects.

MATERIALS AND METHODS

Electroporator

We generated square voltage pulses (5 V) using an AVR microcontroller (ATTINY2313-20PU; Atmel, USA) and amplified it using an operational amplifier (op-amp) (OPA454; Texas Instruments, USA). The control program (C language, deposited at http://sourceforge.net/projects/vivoelec/files/) was compiled with WinAVR (http://winavr.sourceforge.net/) and written to the microcontroller using a USB-connection-type AVR programmer (AVRWRT-3; Kyoritsu Eleshop, Japan). Almost all electronic parts were manually soldered based on our designed electrical diagram (supplementary material Fig. S1). The op-amp was not directly soldered to the circuit board but was attached with a zero-insertion force socket (Kyoritsu Eleshop, Japan) such that only the op-amp chip needs to be exchanged when the output electrodes short-circuit. The power source for driving the op-amp (50-100 V constant voltage) was an electrophoresis power supply (model 500-200; Wakamori, Japan). To prevent the sudden current flux on connection to the power supply, a 10 kΩ variable resistor was inserted between the power supply and the circuit; the resistance was gradually reduced to 0 Ω after connection. The waveform of the amplified square pulses was confirmed using an oscilloscope (LBO-310A; Leader Electronics, Japan), and the voltage amplitude was calibrated using the oscilloscope and power supply.

Insects

B. mori (strain N4) was reared on an artificial diet (NOSAN, Japan) under long-day conditions (16-hour light/8-hour dark) at 25°C. *P. xuthus* was reared on tangerine (*Citrus reticulata*) leaves under long-day conditions at 25°C. *T. castaneum* (strain Ga2) was reared on wholewheat flour containing 5% yeast extract at 30°C.

Vector constructions

DNA vectors (Fig. 1A) were based on pPIGA3GFP (Tamura et al., 2000) (supplementary material Figs S5, S6, Table S2). We first constructed the transitional vector pPIG-A3GG. The partial coding sequence of *actin A3* in the *A3* promoter (*A3*$^{+}$ promoter) was eliminated to yield the *A3* promoter. The fragment containing the entire vector sequence from pPIGA3EGFP and a fragment containing another *EGFP* expression cassette flanked by the *IE2* promoter derived from pIZT-V5/His (Invitrogen, USA) from an unpublished plasmid [that includes the expression cassette between *Sal*I and *Not*I sites of pBluescript KS– (Stratagene, USA)] were amplified by PCR (supplementary material Fig. S5). In-Fusion Enzyme (Takara, Japan) was used to ligate these fragments and for all other ligations, except self-ligations. An unnecessary multiple cloning site was eliminated by *Sma*I and *Sal*I digestion and re-ligation. The redundant *IE2* promoter was excised by *Bst*BI digestion, and the 5′-sequence of the *A3* promoter was amplified from pPIGA3EGFP and cloned into the vector after digestion with *Sal*I. The *A3*$^{+}$ promoter remaining in the plasmid was excised with *Xho*I and *Bam*HI digestion and replaced with another *A3* promoter fragment amplified from pPIGA3GFP to generate pPIG-A3GG.

Department of Integrated Biosciences, Graduate School of Frontier Sciences, The University of Tokyo, Kashiwa, Chiba 277-8562, Japan.

*Author for correspondence (haruh@k.u-tokyo.ac.jp)

Accepted 8 November 2012

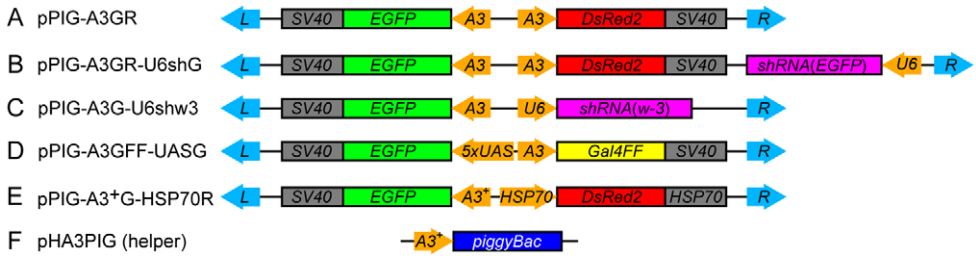

Fig. 1. Schematics of the overexpression cassettes in DNA vectors. (**A**) pPIG-A3GR. (**B**) pPIG-A3GR-U6shG. (**C**) pPIG-A3G-U6shw3. (**D**) pPIG-A3GFF-UASG. (**E**) pPIG-A3G-HSP70R. (**F**) pHA3PIG. Orange arrows, promoters; light-blue arrows, *piggyBac* recognition sites; gray boxes, polyadenylation signals; colored boxes, coding regions.

pPIG-A3GR was obtained by cloning the *DsRed2* ORF cassette from pBac3xP3DsRed2 (Inoue et al., 2005) into *Bam*HI/*Not*I-digested pPIG-A3GG.

pPIG-A3GR-U6shG was obtained by isolating the *U6* promoter fragment flanked with the sequence encoding shRNA against *EGFP* from the *Bombyx* genome (strain p50) using a previously described methods (Wakiyama et al., 2005; Ohtsuka et al., 2008) and cloning it downstream of the *A3/DsRed2/SV40polyA* reporter cassette using *Sfi*I-digested pPIG-A3GR.

pPIG-A3G-U6shw3 was obtained by amplifying the *U6* promoter and shRNA sequence against *w-3* from pPIG-A3GR-U6shG and cloning it into *Xho*I/*Not*I-digested pPIG-A3GG.

pPIG-A3GFF-UASG was obtained by cloning the *Gal4FF* ORF fragment from pT2KhspGFF (Asakawa et al., 2008) into *Bam*HI/*Not*I-digested pPIG-A3GG, excising the *A3* promoter upstream of the *EGFP* ORF with *Xho*I and *Sal*I, and replacing it with the 5×*UAS/HSP70Bb* fragment from pUAST (Brand and Perrimon, 1993).

pPIG-A3^{+}G-HSP70R was a gift from Dr J. Yamaguchi (The University of Tokyo, Japan).

siRNA

siRNA against *EGFP* and *w-3* was designed based on our siRNA design guidelines (Yamaguchi et al., 2011) using the siDirect program (Naito et al., 2009) (http://sidirect2.rnai.jp; supplementary material Table S3) and chemically synthesized and annealed (FASMAC, Japan).

In vivo electroporation

Silkworms and swallowtail butterfly larvae were anesthetized at 4°C before electroporation. Red flour beetle larvae were anesthetized with ethyl ether. After immobilizing the insects with adhesives or forceps, DNA solution (1 μg/μl) was injected into the body cavity using a microinjector (FemtoJet; Eppendorf, Germany) and a broken-tip glass needle (GD-1; Narishige, Japan), which was prepared using a needle puller (PP-830; Narishige) (supplementary material Fig. S3). The larval epidermis and antennal primordium were injected with 0.5 μl of the DNA solution, and the pupal wing was injected with 2.0 μl of the DNA solution. *Tribolium* larvae were injected with the largest possible volume of the DNA solution. Immediately after injection, platinum electrodes were placed near the injection site; on the opposite side of each tissue, PBS droplets were placed nearby and appropriate voltage was applied.

Image collection

All images, except for those of the antenna and wing, were collected from live insects under fluorescence stereomicroscope (Leica M165FC; Germany) using a digital camera (AxioCam MRc5; Carl Zeiss, Germany). The contrast and γ values were adjusted using AxioVision software (release 4.5, Carl Zeiss). Antenna and wing images were collected using fixed tissues (4% paraformaldehyde fixation for 30 minutes at room temperature) under a LASER confocal microscope (FluoView FV1000; Olympus, Japan).

RESULTS AND DISCUSSION

Somatic transgenesis in various tissues of *B. mori*

The optimal voltage for introducing exogenous DNA into tissues *in vivo* of *B. mori* was established using a simple, low-cost electroporator. Unless otherwise stated, different voltages (10-45

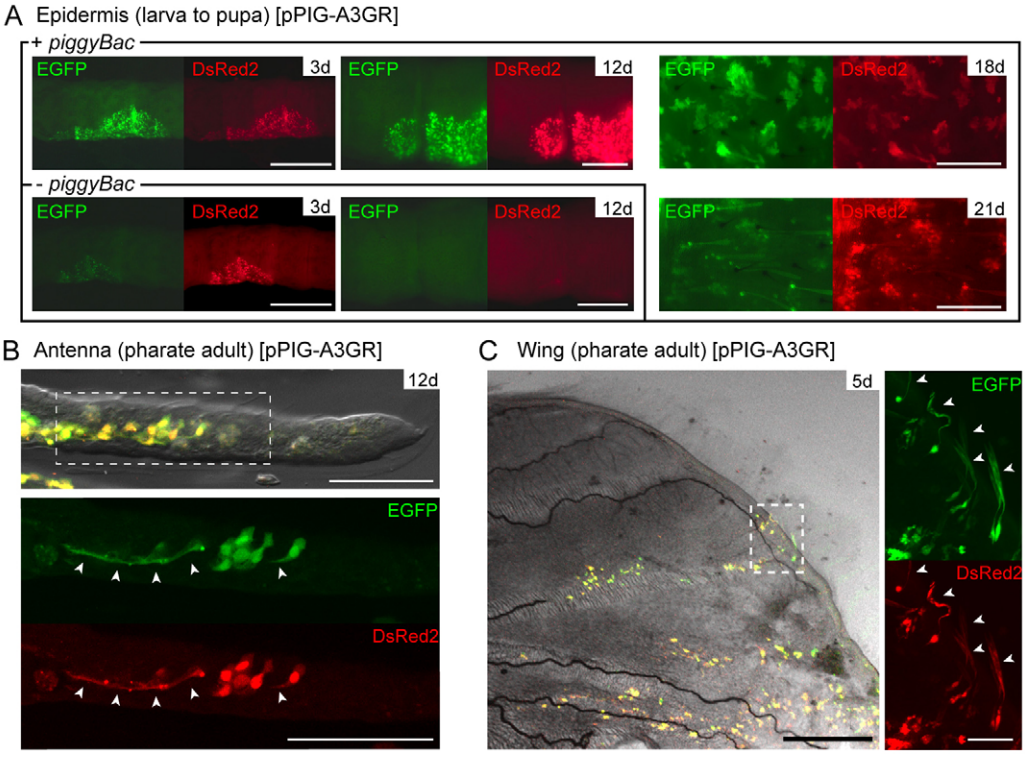

Fig. 2. Overexpression of exogenous genes in various silkworm tissues using *in vivo* electroporation. (**A**) *In vivo* gene transfer into larval epidermis and *piggyBac*-mediated stable expression. Larval abdominal epidermis was electroporated with pPIG-A3GR and pHA3PIG (+*piggyBac*) or with pPIG-A3GR alone (–*piggyBac*). Days post-electroporation are indicated in the upper right corner of each panel; the vector is indicated in brackets next to the caption. (**B**) *In vivo* gene transfer into antennal primordium. Arrowheads indicate transfected olfactory neurons. (**C**) *In vivo* gene transfer into pupal wing. Arrowheads indicate transfected scale cells. Panels in A were photographed under the same conditions; the contrast and γ values of the figures were adjusted in the same manner. Scale bars: 2 mm in A; 100 μm in B and C (right); 500 μm in C (left).

V) were applied for the same duration (five 280 ms pulses per 5 seconds). The target tissues were larval epidermis, antennal primordium and pupal wing.

Plasmid DNA solution was injected into the body cavity near each tissue, and platinum electrodes and droplets of phosphate-buffered saline (PBS) were placed nearby before electroporation (supplementary material Fig. S3). To stably express exogenous genes, we constructed the pPIG-A3GR vector (Fig. 1A) based on the vector used for transgenesis (Tamura et al., 2000). The overexpression cassette of the vector was flanked with the target sequence of the *piggyBac* transposon to be inserted into the chromosome (Fig. 1A-E, 'L' and 'R'). *piggyBac* transposase was supplied by a separate helper plasmid [Fig. 1F, pHA3PIG (helper)]. First, exogenous enhanced green and red fluorescence protein expression (*EGFP* and *DsRed2*) was examined in the larval epidermis (second instar) post-electroporation at 20 V (Fig. 2A). Although the expression was observed 3 days post-electroporation with and without the helper plasmid (Fig. 2A, 3 d), it was still present 12 days post-electroporation only when the vector and the helper plasmid were electroporated together (Fig. 2A, 12 d). Moreover, it was maintained until adulthood (Fig. 2A, + *piggyBac*, 18 d and 21 d). This implied that *piggyBac* facilitated stable expression by generating transgenic somatic cells. Thereafter, the donor and helper plasmids were co-injected in all experiments. Exogenous gene expression was also observed in the antennal primordium (early final instar) post-electroporation with 10 pulses at 45 V and in the pupal wing with five pulses at 20 V. The expression in the antennal primordium was maintained after pupation (12 days post-electroporation), and several cells differentiated into olfactory neurons (Fig. 2B, arrows). In the pupal wing, several cells differentiated into scale cells (Fig. 2C, arrows). Furthermore, several tissues beneath the targeted tissues (e.g. muscle, fat body and trachea) were also transfected in these electroporation treatments, suggesting that functional analyses of various tissue types could be possible using our approach. The survival rates and gene transfer efficiencies are summarized in supplementary material Table S1.

Manipulation of gene expression levels using RNAi and the GAL4/UAS system

Next, we investigated whether RNAi was applicable to this electroporation-mediated system. The *EGFP* gene expressed from a plasmid in the larval epidermis was used as the RNAi target. To stably induce RNAi, we used an RNA polymerase III promoter (*U6* promoter)-driven shRNA (Wakiyama et al., 2005; Ohtsuka et al., 2008). We constructed the pPIG-A3GR-U6shG vector that expressed shRNA against *EGFP* (Fig. 1B) and compared the fluorescence of EGFP with that of pPIG-A3GR. EGFP fluorescence in the DsRed2-positive cells was weaker in all silkworms (compare Fig. 3A and Fig. 2A, n=10), indicating that the shRNA-mediated RNAi system was applicable. We also evaluated the efficacy of direct transfer of siRNA by electroporation. Electroporation of siRNA (400 μM, 0.5 μl) against EGFP weakened the EGFP signal (Fig. 3B, n=10), whereas injection of siRNA did not attenuate this signal (Fig. 3C, n=12). These data indicate that RNAi can be induced by electroporation-mediated direct transfer of siRNA and that our electroporation approach can overcome the low efficiency of introducing siRNA reported in some insects (Tomoyasu et al., 2008; Terenius et al., 2011).

Furthermore, we investigated whether endogenous gene function could be inhibited using these RNAi systems. We focused on the *w-3* gene, which encodes an ABC transporter that regulates accumulation of white pigment in the leucophores in larval silkworm epidermal cells (Quan et al., 2002; Kômoto et al., 2009). Both shRNA-mediated system and direct transfer of siRNA (300 μM, 0.5 μl) mimicked the *w-3* mutant phenotype of translucent skin in the electroporated epidermis (8 d in Fig. 3D,E, arrowheads; n=11 for each), which was not observed in the negative controls (Fig. 3F, n=16; supplementary material Fig. S4). However, these two systems resulted in different phenotypic patterns. shRNA-

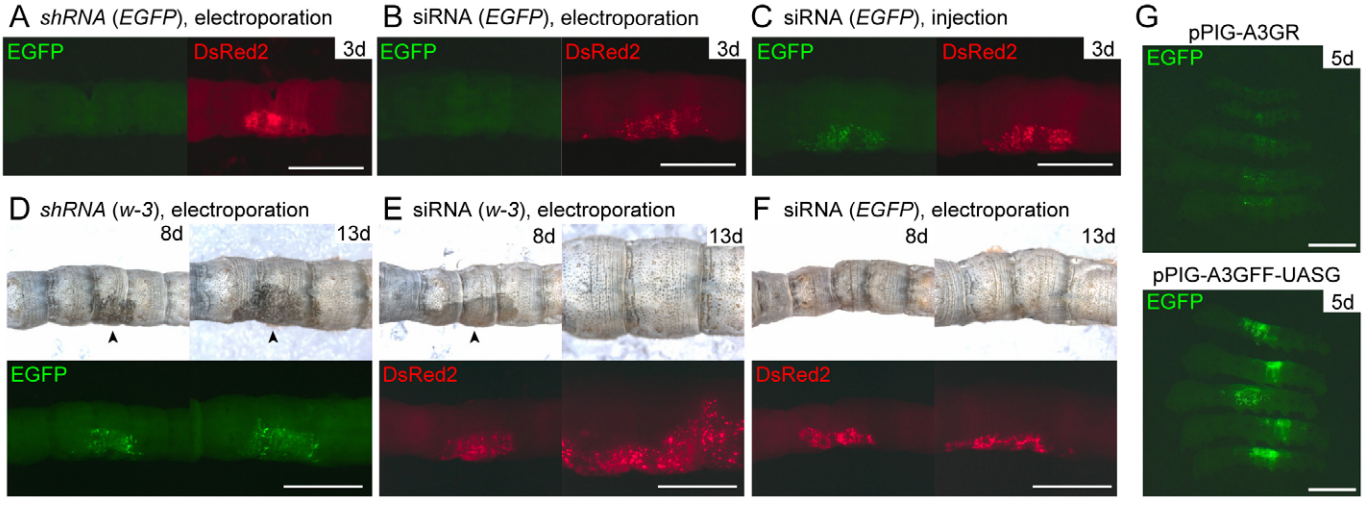

Fig. 3. Manipulation of gene expression levels using RNAi and the *Gal4/UAS* system. (A-C) Downregulation of artificially expressed *EGFP* by RNAi. Days post-electroporation are indicated in the upper right corner of each panel. (**A**) Downregulation of *EGFP* by shRNA using pPIG-A3GR-U6shG. (**B**) Downregulation of *EGFP* by shRNA. (**C**) Larva injected with siRNA against *EGFP* 1 hour post-electroporation of pPIG-A3GR. Larval fluorescence in A-C was photographed and adjusted as in Fig. 2A. (D-F) Downregulation of endogenous *w-3* expression by RNAi. Upper panels, bright field; lower panels, reporter gene expression from simultaneously transfected cassettes (*EGFP*, *DsRed2*). (**D**) Downregulation of *w-3* by shRNA using pPIG-A3G-U6shw3. (**E**) Downregulation of *w-3* by siRNA. Translucent skin is indicated by arrowheads in D,E. (**F**) Electroporation of negative-control (*EGFP*) siRNA. pPIG-A3GR was simultaneously electroporated as a reporter in E,F. (**G**) Dose control of an exogenous gene using the *GAL4/UAS* system. Five larvae electroporated with each vector are shown. Scale bars: 2 mm in A-C; 5 mm in D-G.

mediated RNAi induced mosaic translucent skin that was maintained until the final instar (Fig. 3D, arrows), whereas direct siRNA transfer induced a broader translucent region (Fig. 3E, 8 d, arrow), which reduced over time (Fig. 3E, 13 d). These data suggest that the transgenesis-based RNAi system is suitable for inducing RNAi for prolonged periods and that direct siRNA transfer could be useful for testing short-term effects.

Evaluating the effects of gene product dose on phenotype is also important for analyzing gene function. To increase transcriptional efficiency, we constructed the pPIG-A3GFF-UASG vector (Fig. 1D) that uses the strong transcriptional activity of the *GAL4/UAS* system (Brand and Perrimon, 1993). Using this vector, we observed an increase in the levels of the exogenous gene product (Fig. 3G; n=5). Further manipulation of transcriptional activity with the *GAL4/UAS* system, such as modifying the number of *UAS* repeat sequences, should enable fine-tuning of the dosage.

Electroporation-mediated somatic transgenesis in other insects

We investigated whether our electroporation procedure was applicable to a broader range of insect species. We used pPIG-A3^{+}G-HSP70R (Fig. 1E), in which reporter genes are driven by two different promoters active in non-host insects: *BmA3*, honey bee (Ando et al., 2007); *DmHSP70*, beetle, butterfly and silk moth (Oppenheimer et al., 1999; Ramos et al., 2006; Uhlirova et al., 2002). With the *HSP70* promoter, we observed a leaky promoter activity under standard rearing conditions. We first tested the swallowtail butterfly *P. xuthus* as a species relatively closely related to *B. mori*. As *P. xuthus* displays two different mimicry body patterns on the larval epidermis during development, it is suitable for analyzing molecular mechanisms of mimicry and its evolution (Futahashi and Fujiwara, 2008) (Fig. 4A, left). We conducted electroporation in the same manner as for *B. mori* larval epidermis. Exogenous gene expression was observed with both promoters (20 V, second instar treatment) and was maintained even after a change in body color (Fig. 4A, 14 d, 17 d; n=1). Simultaneous electroporation of siRNA against *EGFP* (30 V, third instar treatment) attenuated *EGFP* expression in *P. xuthus* (Fig. 4B, dotted square; n=2), suggesting that transposon-mediated stable expression and direct transfer of siRNA are applicable to *P. xuthus*.

We subsequently tested the red flour beetle *T. castaneum* as a species more distantly related to *B. mori*. We electroporated the larvae before the last instar in essentially the same manner as described above (20 V, 5 pulses). Seven days post-electroporation, EGFP fluorescence was primarily observed in muscles, and DsRed2 fluorescence was observed in a subset of the EGFP-positive tissues (Fig. 4C, 7 d). The lower DsRed2 signal may be attributed to the low core activity of *DmHSP70* promoter reported in this insect (Schinko et al., 2010). However, both of the fluorescence signals were maintained even after pupation (Fig. 4C, 11 d, arrows; n=7). These data suggest that a stable expression of *piggyBac* can also be achieved in *Tribolium*. The survival rates and gene transfer efficiencies in these insects are listed in supplementary material Table S1.

Conclusions

Our electroporation-mediated approach enabled gain-of-function and loss-of-function analyses in various tissues of three insect species, including two non-model insects. Using the *piggyBac* transposon, stable transgenic somatic cells were generated within different tissues at various developmental stages. In this system, the time from experimental design to obtaining results is very short; therefore, functional analyses of many genes in non-model insects may become possible. Generation of genetic mosaics will allow functional analyses of embryonically lethal signaling molecules and the study of neighboring cell interactions in non-model insects. We believe that this method could be a powerful tool for developmental genetic analyses in insects.

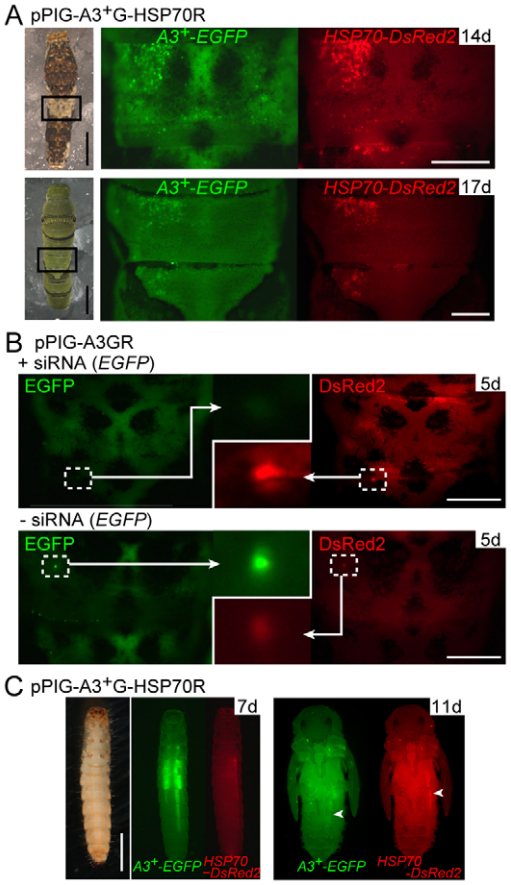

Fig. 4. Electroporation-mediated gene transfer in the swallowtail butterfly and red flour beetle. (**A**) Overexpression in *P. xuthus*. Left, bright-field images; right, fluorescent images within the range of the rectangles in the bright field. (**B**) Attenuation of *EGFP* expression through simultaneous electroporation of siRNA against *EGFP*. Reporter plasmid pPIG-A3GR was electroporated with or without siRNA against *EGFP* (+siRNA and −siRNA, respectively). The central images are enlargements of the outlined areas. (**C**) Overexpression of EGFP and DsRed in *T. castaneum* at 7 and 11 days post-electroporation. Left-hand images show a larva 7 days post-electroporation (left, bright field; right, fluorescent). Right-hand fluorescent images show the pupated larva 11 days post-electroporation. Plasmids are indicated at the top of the figures. Scale bars: 5 mm in A (left); 1 mm in A (right); 1 mm in B,C.

Acknowledgements

We thank Dr T. Tamura (National Institute of Agrobiological Sciences, Japan) for providing us plasmids pHA3PIG, pPIGA3GFP and pBac3xP3DsRed2; Dr K. Kawakami (National Institute of Genetics, Japan) for plasmid pT2KhspGFF; and Drs T. Kojima and J. Yamaguchi (The University of Tokyo, Japan) for helpful discussion.

Funding

This work was supported by Grant-in-Aid for Scientific Research on Priority Areas 'Comparative Genomics' from the Ministry of Education, Culture, Sports, Science and Technology of Japan [20017007 to H.F.], and Grants-in-Aid for Scientific Research [22128005 to H.F.].

Competing interests statement
The authors declare no competing financial interests.

Author contributions
T.A. conceived the concept; T.A. and H.F. designed the experiments; T.A. established the electroporation system and performed all experiments; T.A. and H.F. wrote the manuscript.

Supplementary material
Supplementary material available online at
http://dev.biologists.org/lookup/suppl/doi:10.1242/dev.085241/-/DC1

References
Ando, T., Fujiyuki, T., Kawashima, T., Morioka, M., Kubo, T. and Fujiwara, H. (2007). In vivo gene transfer into the honeybee using a nucleopolyhedrovirus vector. *Biochem. Biophys. Res. Commun.* **352**, 335-340.
Asakawa, K., Suster, M. L., Mizusawa, K., Nagayoshi, S., Kotani, T., Urasaki, A., Kishimoto, Y., Hibi, M. and Kawakami, K. (2008). Genetic dissection of neural circuits by Tol2 transposon-mediated Gal4 gene and enhancer trapping in zebrafish. *Proc. Natl. Acad. Sci. USA* **105**, 1255-1260.
Brand, A. H. and Perrimon, N. (1993). Targeted gene expression as a means of altering cell fates and generating dominant phenotypes. *Development* **118**, 401-415.
Futahashi, R. and Fujiwara, H. (2008). Juvenile hormone regulates butterfly larval pattern switches. *Science* **319**, 1061.
Inoue, S., Kanda, T., Imamura, M., Quan, G. X., Kojima, K., Tanaka, H., Tomita, M., Hino, R., Yoshizato, K., Mizuno, S. et al. (2005). A fibroin secretion-deficient silkworm mutant, Nd-s^{D}, provides an efficient system for producing recombinant proteins. *Insect Biochem. Mol. Biol.* **35**, 51-59.
Kômoto, N., Quan, G. X., Sezutsu, H. and Tamura, T. (2009). A single-base deletion in an ABC transporter gene causes white eyes, white eggs, and translucent larval skin in the silkworm w-3(^{oe}) mutant. *Insect Biochem. Mol. Biol.* **39**, 152-156.
Moczek, A. P. and Rose, D. J. (2009). Differential recruitment of limb patterning genes during development and diversification of beetle horns. *Proc. Natl. Acad. Sci. USA* **106**, 8992-8997.
Naito, Y., Yoshimura, J., Morishita, S. and Ui-Tei, K. (2009). siDirect 2.0: updated software for designing functional siRNA with reduced seed-dependent off-target effect. *BMC Bioinformatics* **10**, 392.
Ohtsuka, D., Nakatsukasa, T., Fujita, R., Asano, S., Sahara, K. and Bando, H. (2008). Use of Bombyx mori U6 promoter for inducing gene-silencing in silkworm cells. *J. Insect Biotechnol. Sericology* **77**, 125-131.
Oppenheimer, D. I., MacNicol, A. M. and Patel, N. H. (1999). Functional conservation of the wingless-engrailed interaction as shown by a widely applicable baculovirus misexpression system. *Curr. Biol.* **9**, 1288-1296.
Quan, G. X., Kanda, T. and Tamura, T. (2002). Induction of the white egg 3 mutant phenotype by injection of the double-stranded RNA of the silkworm white gene. *Insect Mol. Biol.* **11**, 217-222.
Ramos, D. M., Kamal, F., Wimmer, E. A., Cartwright, A. N. and Monteiro, A. (2006). Temporal and spatial control of transgene expression using laser induction of the hsp70 promoter. *BMC Dev. Biol.* **6**, 55.
Schinko, J. B., Weber, M., Viktorinova, I., Kiupakis, A., Averof, M., Klingler, M., Wimmer, E. A. and Bucher, G. (2010). Functionality of the GAL4/UAS system in Tribolium requires the use of endogenous core promoters. *BMC Dev. Biol.* **10**, 53.
Tamura, T., Thibert, C., Royer, C., Kanda, T., Abraham, E., Kamba, M., Komoto, N., Thomas, J. L., Mauchamp, B., Chavancy, G. et al. (2000). Germline transformation of the silkworm Bombyx mori L. using a piggyBac transposon-derived vector. *Nat. Biotechnol.* **18**, 81-84.
Terenius, O., Papanicolaou, A., Garbutt, J. S., Eleftherianos, I., Huvenne, H., Kanginakudru, S., Albrechtsen, M., An, C., Aymeric, J. L., Barthel, A. et al. (2011). RNA interference in Lepidoptera: an overview of successful and unsuccessful studies and implications for experimental design. *J. Insect Physiol.* **57**, 231-245.
Tomoyasu, Y., Wheeler, S. R. and Denell, R. E. (2005). Ultrabithorax is required for membranous wing identity in the beetle Tribolium castaneum. *Nature* **433**, 643-647.
Tomoyasu, Y., Miller, S. C., Tomita, S., Schoppmeier, M., Grossmann, D. and Bucher, G. (2008). Exploring systemic RNA interference in insects: a genome-wide survey for RNAi genes in Tribolium. *Genome Biol.* **9**, R10.
Uhlírová, M., Asahina, M., Riddiford, L. M. and Jindra, M. (2002). Heat-inducible transgenic expression in the silkmoth Bombyx mori. *Dev. Genes Evol.* **212**, 145-151.
Wakiyama, M., Matsumoto, T. and Yokoyama, S. (2005). Drosophila U6 promoter-driven short hairpin RNAs effectively induce RNA interference in Schneider 2 cells. *Biochem. Biophys. Res. Commun.* **331**, 1163-1170.
Yamaguchi, J., Mizoguchi, T. and Fujiwara, H. (2011). siRNAs induce efficient RNAi response in Bombyx mori embryos. *PLoS ONE* **6**, e25469.

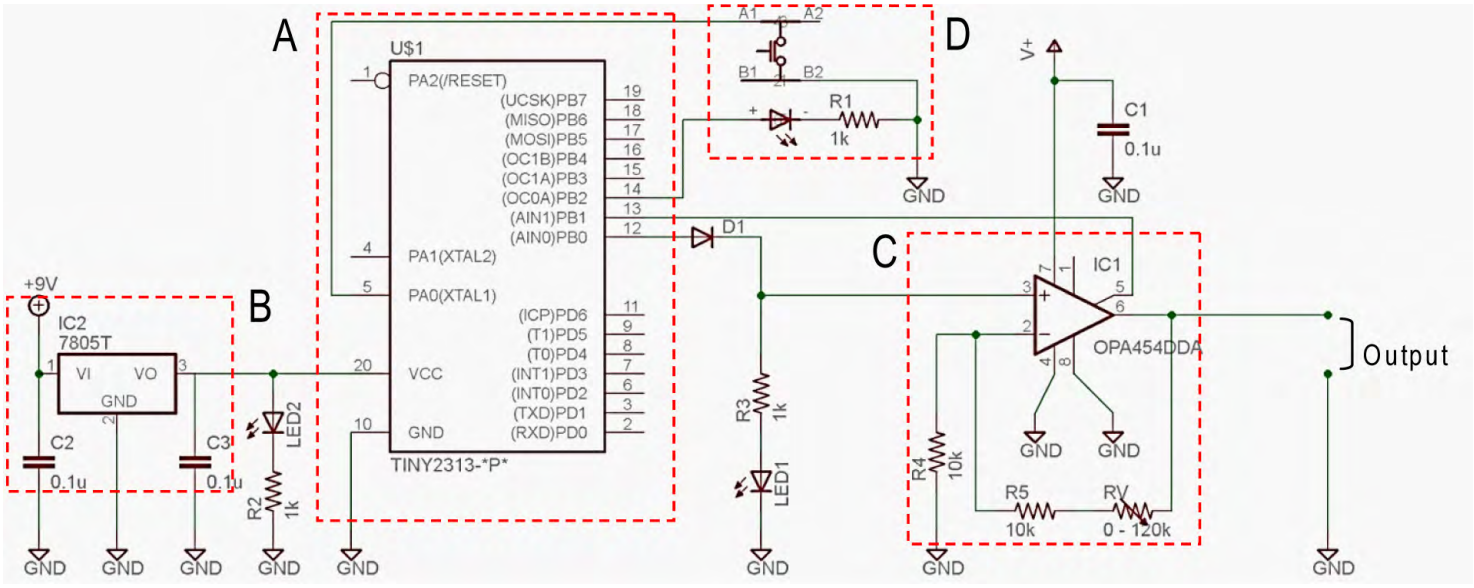

Fig. S1. Electronic circuit of the electroporator. (**A**) AVR microcontroller. (**B**) Power supply unit for AVR. (**C**) Operational amplifier unit. (**D**) LED-containing push switch unit. C1-C3, capacitor; R1-R5 and RV, resistor; D1, diode; GND, ground.

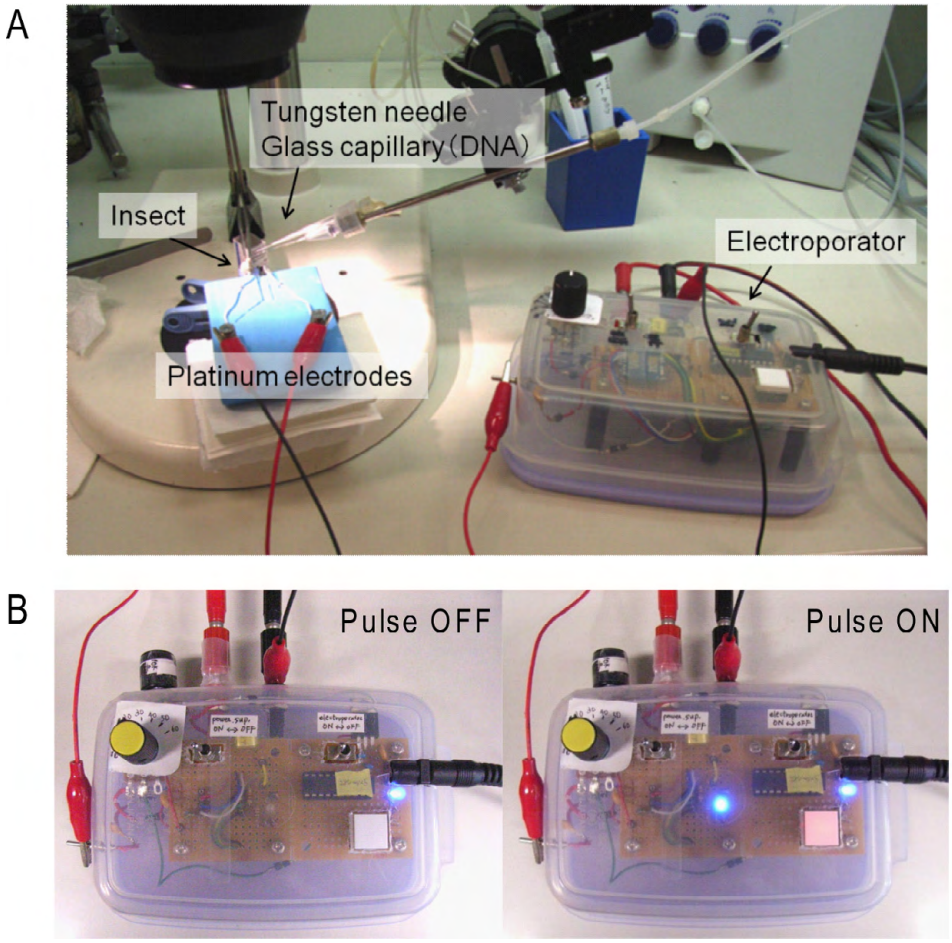

Fig. S2. Overview of the *in vivo* electroporator. (**A**) A set of *in vivo* electroporation apparatuses. (**B**) Overview of the electroporator while applying voltage pulses. Voltage status can be monitored with lighting of the LED.

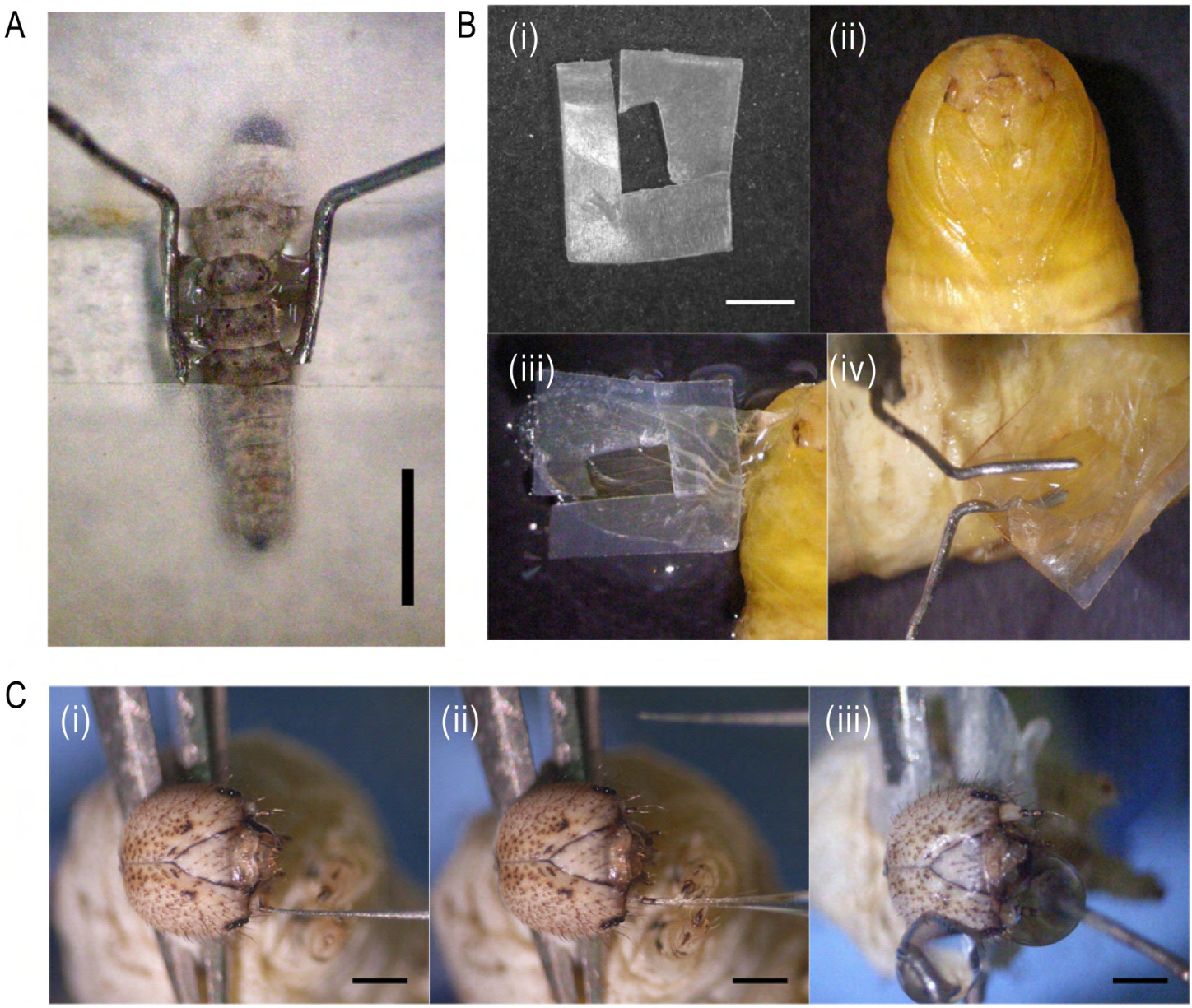

Fig. S3. Procedures of *in vivo* electroporation for each tissue. (**A**) Gene transfer to larval epidermis. After injecting DNA solution, platinum electrodes and droplets of PBS were placed near the injection site, and voltage pulses were applied. Scale bar: 2 mm. (**B**) Gene transfer to pupal wing. (i) A Parafilm gasket was prepared to be inserted between a fore wing and a hind wing. (ii) A pupa that had just pupated was selected. (iii) The fore wing was floated on water and the gasket was placed on the ventral side of the wing. (iv) After wiping water droplets from the body surface, DNA solution was injected into the hemocoel of the forewing. The platinum electrodes and droplets of PBS were placed on both the ventral and dorsal sides of the wing and voltage pulses were applied. Scale bar: 1 mm. (**C**) Gene transfer to antennal primordium. (i) A larval head was grasped with forceps and the tip of the larval antenna was pierced with a sharp tungsten needle. The tungsten needle was prepared using electrolytic grinding (ii) DNA solution was injected through the hole. (iii) Platinum electrodes and droplets of PBS were placed as above and voltage pulses were applied. Scale bars: 1 mm.

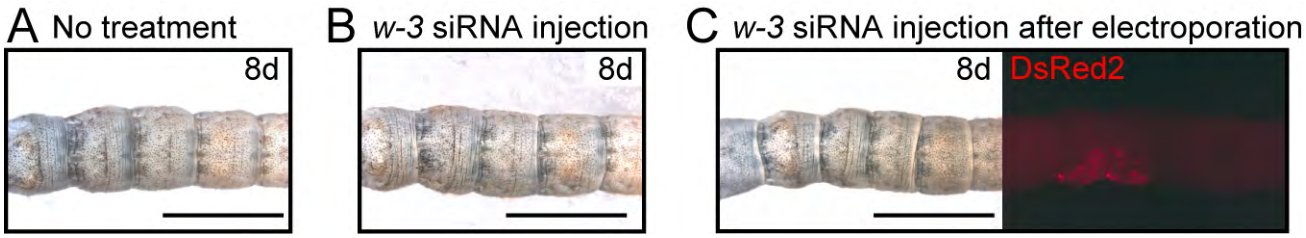

Fig. S4. Negative control experiments for RNAi against *w-3*. (**A**) No treatment (*n*=10). (**B**) *w-3* siRNA injection (300 μM, 0.5 μl) (*n*=10). (**C**) *w-3* siRNA injection (300 μM, 0.5 μl) 1 hour after electroporation of pPIG-A3GR (*n*=6). Left, bright field; right, DsRed2 signal. Images were collected 8 days after each treatment. No attenuation of white pigmentation was observed under each condition. Scale bar: 5 mm.

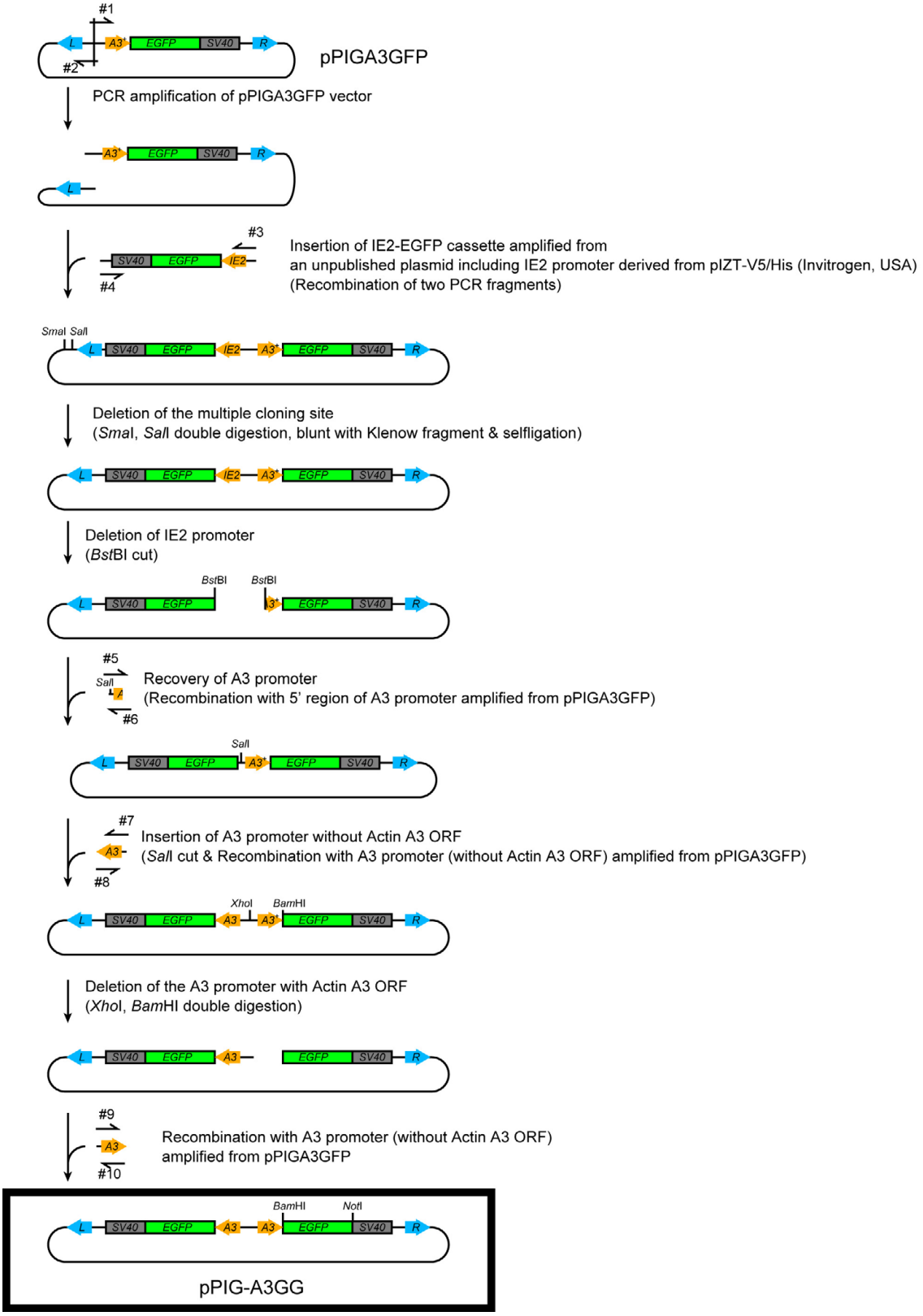

Fig. S5. Construction of the pPIG-A3GG transitional vector. pPIG-A3GG was constructed based on pPIGA3GFP (Tamura et al., 2000). Each step is indicated next to each arrow. When a PCR fragment was added, the structure of the amplified fragment and primer number are shown together. Primer sequences (#1-#10) are listed in supplementary material Table S2.

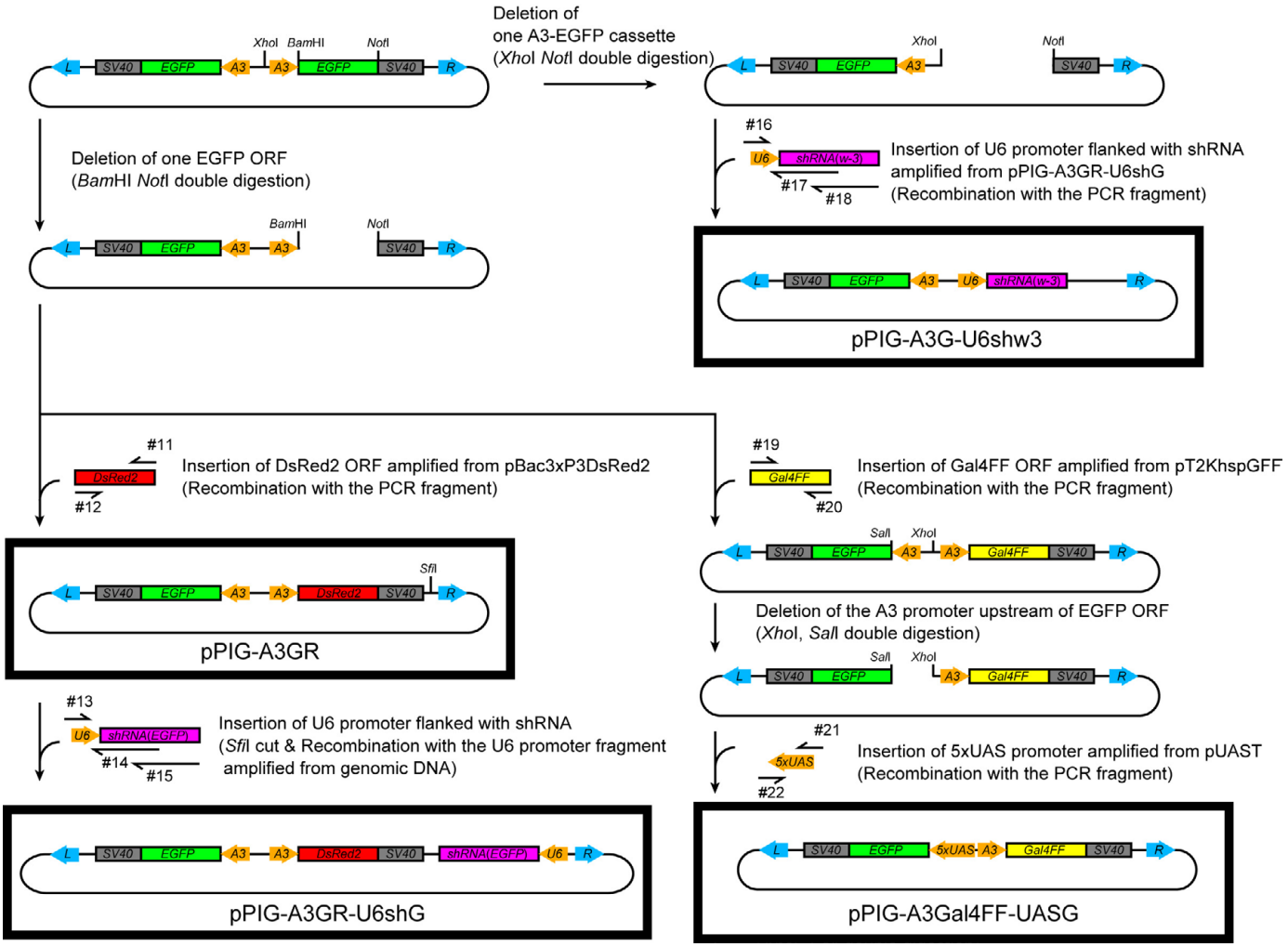

Fig. S6. Construction of donor vectors. pPIG-A3GR, pPIG-A3GR-U6shG, pPIG-A3G-U6shw3 and pPIG-A3GFF-UASG were based on the transitional vector pPIG-A3GG (supplementary material Fig. S4). Each step is indicated next to each arrow. When a PCR fragment was added, the structure of the amplified fragment and primer number are shown together. Primer sequences (#11-#22) are listed in supplementary material Table S2.

Table. S1. Electroporation conditions, survival rate and gene transfer efficiency

Insect species	Target tissue	Electroporation condition	Survival rate (5 days after electroporation)	Fluorescence signal in the survived (5 days after electroporation)	Notes
Bombyx mori	Larval epidermis	45V, 280ms/1s, 5 pulses (2nd instar)	0/15 (0%)	–	The larvae in the experiments for Fig. 2A (+ *piggyBac*) were counted.
		45V, 280ms/1s, 5 pulses (3rd instar)	2/4 (50%)	2/2 (100%)	The larvae in the experiments for Fig. 2A (+ *piggyBac*) were counted.
		20V, 280ms/1s, 5 pulses (2nd instar)	11/21 (52%)	11/11 (100%)	The larvae in the experiments for Fig. 2A (+ *piggyBac*) were counted.
	Pupal wing	45V, 280ms/1s, 5 pulses	2/2 (100%)	0/4 (0%)*	The larvae in the experiments for Fig. 2B were counted.
		30V, 280ms/1s, 5 pulses	4/4 (100%)	0/4 (0%)*	The larvae in the experiments for Fig. 2B were counted.
		20V, 280ms/1s, 5 pulses	4/4 (100%)	2/4 (50%)*	The larvae in the experiments for Fig. 2B were counted.
	Antennal primordium	45V, 280ms/1s, 10 pulses	13/20 (65%)	11/13 (85%)	The larvae in the experiments for Fig. 2C were counted.
		20V, 280ms/1s, 5 pulses	4/4 (100%)	0/4 (0%)	The larvae in the experiments for Fig. 2C were counted.
Papilio xuthus	Larval epidermis	20V, 280ms/1s, 5 pulses (2nd instar)	1/3 (33%)	1/1 (100%)	The larvae in the experiments for Fig. 4A were counted.
		30V, 280ms/1s, 5 pulses (3rd instar)	3/5 (60%)	3/3 (100%)	Both larvae treated with and without siRNA (n = 2 and 3, respectively) in the experiments for Fig. 4B were counted together.
Tribolium castaneum	Larval abdomen	20V, 280ms/1s, 5 pulses	7/11 (64%)	7/7 (100%)	The larvae in the experiments for Fig. 4C were counted.

*Insects with fluorescent scale cells were counted

Table. S2. The PCR primers used for vector constructions

Primer	Sequence (5'-3')
#1	cagaggactattagaggtaagaataaac
#2	tggcaaggtcaagattctgttagaag
#3	tctaatagtcctctggatcatgatgataaacaatgtatggtgc
#4	atcttgaccttgccatttatttgtaaccattataagctgcaat
#5	gctcaccatggttcggtcgaccagaggactattagaggtaa
#6	gacggagaaccttcgaaattc
#7	tagtcctctggtcgatcgcgttaccatatatggtg
#8	ccatggttcggtcgaccttgaattagtctgcaagaaaag
#9	attgtcagatctcgagctca
#10	ggcgaccggtggatccttgaattagtctgcaagaaaag
#11	tctagagtcgcggccgct
#12	actcgtacggggatccaccggtcgccaccatggcctcctccgagaacgt
#13	atagctcagaggccgagaatttttcaaatcggaccag
#14	gaggacagcacactcttgaaattcaccttaatacacttgataatctttttattttgga
#15	cagaggccgaggccgaaaaagcatcaaggtgaacttcaagaggacagcacactcttgaaattca
#16	attgtcagatctcgaagaatttttcaaatcggaccag
#17	ggggacagcacacctttcaatacctatataacaacttgataatctttttattttgga
#18	tctagagtcgcggccgcaaaaacgttatacaggtactgaaaggggacagcacacctttcaatacc
#19	actaattcaaggatctccgcggcgccaccatgaagctactgtcttctatcgaac
#20	tctagagtcgcggccaggcctttagttacccgggagcatat
#21	caagcttgagctcgactcgcgagcatgcctgcaggtcggagt
#22	gacctgcaggcatgcatttaaattccgatccagacatgataagatacat

Table. S3. siRNA sequences

Target gene	Direction	Sequence (5'-3')
EGFP	Sense	GCAUCAAGGUGAACUUCAAGA
	Antisense	UUGAAGUUCACCUUGAUGCCG
w-3	Sense	CAUUUAUGGCCCAAAACGUUA
	Antisense	ACGUUUUGGGCCAUAAAUGAA